



# Eddy current evaluation for thickness loss estimation of aluminum alloys used in aircraft structures

Seekharin KOMONHIRUN<sup>1</sup>, Sujittra TANGPRAKOB<sup>1</sup>, Sorawit CHANAPHAN<sup>1</sup>, Awika JAROENSRI<sup>1</sup>, Thanasak NILSONTHI<sup>2</sup>, and Thammaporn THUBLAOR<sup>2,\*</sup>

<sup>1</sup> Department of Power Engineering Technology, College of Industrial Technology, King Mongkut's University of Technology North Bangkok, Thailand

<sup>2</sup> High Temperature Corrosion Research Centre, Department of Materials and Production Technology Engineering, Faculty of Engineering, King Mongkut's University of Technology North Bangkok, Thailand

\*Corresponding author e-mail: Thammaporn.t@eng.kmutnb.ac.th

## Received date:

31 December 2022

## Revised date

22 June 2023

## Accepted date:

22 June 2023

## Keywords:

Non-destructive testing;  
Eddy current evaluation;  
Corrosion

## Abstract

Aluminum alloys are commonly used in the aircraft industry but it tends to corrode and needs to be inspected properly. Eddy current testing is the widely used non-destructive testing (NDT) for aircraft metals. This research studied estimating the thickness loss due to corrosion in an aircraft aluminum sheet metal. The Al1100, Al2024, and Al7075 were 2 mm thick. Aluminum sheet metals were used to create artificial damage in hydrochloric acid. The thickness loss due to corrosion was inspected with eddy current testing (ET) and compared with the measurement from the coordinate measurement machine (CMM). The results showed that the thickness loss due to corrosion could be estimated using the eddy current skin depth frequencies. However, in the practical application, the skin depth could be guessed from the corrosion rate which could reduce the inspection time. In this research, the corrosion rate was measured by using potentiodynamic measurement. It can be used for estimating the thickness loss for an appropriate inspection interval.

## 1. Introduction

Various aluminum types are used in modern civil aircraft these days. Aluminum grade 2024 and 7075 are commonly used in aircraft structures for example aircraft skin, frames, stringers, floor beams, and longerons. However, under routine flight usage, the aluminum tends to corrode quickly and needs to be inspected to ensure the safety of flight [1]. The small or shallow corrosion can spread quickly if that part remains unchecked for a long time or due to an inappropriate inspection schedule [2].

The corrosion can be identified from a material or thickness loss due to corrosion. The non-destructive testing (NDT) methods are used to detect damage and determine thickness loss due to corrosion. Consider the aircraft skin which is aluminum sheet metal, if the corrosion were located on the top surface, it could be inspected by visual or other Non-destructive testing (NDT) methods [3-5]. But if the corrosion were hidden or located on the opposite side of the surface, it would be difficult to inspect properly. The NDT method that could be appropriate to inspect the aluminum corrosion in this circumstance is eddy current testing [6,7].

Eddy current testing is categorized as a surface method. The defects that are normally identified by this method are included surface crack, scratch, nick, and corrosion [8-11]. However, this method can inspect sub-surface defects if using the correct probe frequencies.

The eddy current uses alternating current that flows through the excitation copper coil inside the probe to produce an alternated magnetic flux. When using a probe to inspect the conductive workpiece, these magnetic fluxes permeate into the workpiece surface and generate eddy current. The defect is the disturbance of eddy current. This also affects the change of magnetic flux linkage between the workpiece and the probe, sensing by the measuring coil. Then the signal is sent and displayed as voltage, current or impedance changes.

The eddy current has the highest strength at the top surface that contact with the probe. The eddy current strength is decreasing exponentially inside the materials due to the conductivity, magnetic permeability of materials, and frequencies of probe. According to skin effect theory, the higher frequencies usage push the eddy current to the top surface near the probe which can identify the shallow defects but the low frequencies pull the eddy current deep into the workpiece appropriate for detecting deeper or sub-surface defects. However, to detect the corrosion on the opposite side of the sheet metal surface, a very low frequency probe such as a reflection probe is recommended.

In this research, artificial corrosion damages are produced to simulate the corrosive thickness loss by using electro-etching technique. The thickness loss from these artificial damages is inspected by eddy current testing with a reflection probe. The signal amplitudes are analyzed to estimate the thickness loss according to skin effect theory and compared with thickness loss measurement from a coordinate

measuring machine (CMM). Then the results are compared with the corrosion rate (mm/year) from potentiostat-galvanostat instrument to estimate the appropriate inspection schedule.

## 2. Experimental

### 2.1 Artificial corrosion damage

This research considers three types of aluminium sheets, Al1100, Al2024, and Al7075. The Al1100 is represented the pure aluminium (Al 99% and Cu 0.12 wt%). The Al2024 (Al 93.5%, Cu 4.4%, Mn 0.6% and Mg 1.5 wt%), and Al7075 (Al 89%, Cu 2.3%, Mg 2.3%, Cr 0.23%, Zn 6.2%, and Zr 0.12 wt%) are aircraft aluminum that is normally used for fuselage and wing structure. Al1100 sheet metal is considered a non-heat treatment condition but Al2024 and Al7075 are heat treatment at T3 and T6 conditions respectively. Al2024 T3 sheet is aging at a temperature between 185°C to 195°C with 10 h holding time. Al7075 T6 sheet is aging between 157°C to 168°C with 24 h to 30 h holding time. The samples were cut to 3 cm × 12 cm with 2 mm thick. The samples were ground with sandpaper up to 1000 grit and cleaned by an ultrasonic cleaner for 5 min, and dried with a hot air blower. A direct current (DC) power supply was used to create the corrosion damage. The sample was etched with 0.6 M hydrochloric acid in a 1.5 cm hole dimension. The penetration depth of corrosion damage was controlled by time etch according to Faraday's law. The various time was divided into 1 min to 9 min at a constant apply current of 1 A. Photographs of the corrosion damage with different etching times were demonstrated in Figure 1. There are three different corrosion depths for each sample plate. The first plate (A1) contains 1, 2, and 3 min of corrosion time damage. Next, the second plate (A2) contains 4, 5, and 6 min and the third plate (A3) contains 7, 8, and 9 min of damage. Three samples were prepared in each condition. After the damage caused by corrosion each time, the weight loss was recorded by a five-digit semi-micro balance.

After the corrosion generator process, all artificial corrosion damages were measured in the thickness loss by using a coordinate measuring machine (CMM) model LH 54 standard with 0.1 μm resolution. The pneumatic system CMM was used to maintain the measuring table level coordinate during the measuring process.



**Figure 1.** Photograph of the artificial corrosion damage with different etching times.

Before the measurement begins, all sample plates were cleaned with alcohol to remove undesirable dust and left for 15 min and maintained the workpiece temperature. Then, the measuring probe was used to measure the penetration depth at different coordinates between the damage and the near surface to calculate the thickness loss and recorded the data. Finally, the measuring results from the four sets of samples were averaged.

### 2.2 Corrosion rate identification

The polarization technique was used to measure the corrosion rate in 0.6 mol·dm<sup>-3</sup> NaCl solution. The electrochemical cell was a polyvinyl chloride (PVC) cylinder with a sample hole area of 0.785 cm<sup>2</sup> at the bottom cell. This method consists of three electrodes pairing with each other. The first electrode was the working electrode that contact with the sample. The platinum rod was used as a counter electrode and the reference electrode was a silver/silver chloride (Ag/AgCl) electrode. In the beginning, the sample was subjected to open circuit potential (OCP) for 30 min and a scan rate of 1 mV·s<sup>-1</sup>. The sample was polarized within the range of -700 mV and +800 mV with respect to OCP. At least three trials for each condition were carried out. The corrosion current density ( $i_{corr}$ ) was determined by intersecting a cathodic Tafel line with an anodic Tafel line. The potential at the intersection was corrosion potential ( $E_{corr}$ ). The corrosion rate (CR) is calculated by using the following Equation (1) [16]:

$$CR(\text{mm/y}) = 3268.5 \frac{i_{corr} EW}{\rho} \quad (1)$$

where  $i_{corr}$  was the corrosion current density (A·cm<sup>-2</sup>), EW was the equivalent weight of sample (g·mol<sup>-1</sup>) [16] and  $\rho$  was the density of sample (g·cm<sup>-3</sup>) [17].

### 2.3 Eddy current inspection process

In this process, the damages are inspected using Mentor EM, eddy current inspection device. The display of this device was presented in an impedance plane, which demonstrated the impedance change graphic from the measuring coil. The reflection probe with a probe frequency of 300 Hz to 100 kHz was used to inspect the corrosion damage. Before inspection, the frequency in each case much be calculated from Equation (2) [18,19].

$$f = \frac{1}{\pi \mu \sigma \delta^2} \quad (2)$$

$\sigma$  was conductivity in MS·m<sup>-1</sup> unit or it can also use the International Anneal Copper Standard (%IACS). The conductivities were varied in each material.  $\mu$  was the magnetic permeability which is the multiple of relative magnetic permeability of material (1 for non-ferromagnetic material) and magnetic permeability of vacuum that is equal to  $4\pi \times 10^{-7}$  H·m<sup>-1</sup> and  $\delta$  is depth of penetration or skin depth in distance unit. The depth of penetration was set at 2 mm equal to sheet metal thickness. The conductivity of Al1100, Al2024 and Al7075 were listed as 59.5, 32.5 and 32% IACS then the first inspection frequencies are 1.811 kHz, 3.316 kHz and 3.367 kHz, respectively.

The difference in the first inspection frequency caused by the different material properties, such as conductivity in each material. At the same time, the depth of penetration is set equally at a material thickness (2 mm). For other parameters such as gain, phase and sampling rate were adjusted appropriately according to frequency usage.

### 3. Results and discussion

#### 3.1 Artificial damage measurement results

After electrochemical etching, mass loss results of each material type were averaged and demonstrated graphically in Figure 2. It was found that mass loss of all samples tended to be similar in the range of 1 min to 6 min of etching time. The Al2024 results were resembled the Al7075 with slightly lower mass loss at 0.067 g. The lowest mass loss was the Al1100 at 0.06 g. From this result, it is concluded that the Al1100 has a higher corrosion resistance than Al2024 and Al7075, respectively.

For thickness loss measurement from CMM, the average results were shown in Figure 3. It was found that, the thickness loss measurement was found to have the same trend as the mass loss results. However, the results slightly resemble each other due to the roughness of the corrosion surface. Notice that at the corroded surface of Al7075 and Al2024, there were the black dust which cannot be removed completely

by the cleaning process. This black dust was the result of the copper (II) oxide (CuO) which form the Al-Cu cluster from both materials that contain the higher copper composition [20].

#### 3.2 Corrosion rate results from potentiostat/galvanostat instrument

The results of three different aluminium alloys from the linear potentiodynamic polarization technique were shown in Figure 4. The corrosion potential ( $E_{corr}$ ) is a potential value at the lowest current density in cathodic zone. The corrosion potential of Al7075 was lower than that Al2024 and Al1100 at values of -990 mV, -750 V, and -740 V, respectively.

The corrosion current density ( $i_{corr}$ ) is a corrosion rate which is related to the corrosion resistance of sample. Corrosion current density is a current value per area at Cathodic Tafel line interest with Anodic Tafel line. It was found that, the Al1100 showed the lowest corrosion rate at  $2.11 \times 10^{-6} \text{ A}\cdot\text{cm}^{-2}$  and Al7075 showed the highest at  $5.49 \times 10^{-6} \text{ A}\cdot\text{cm}^{-2}$ . Moreover, these results can calculate corrosion rate in terms of thickness loss per time (mm/year) as summarized in Table 1. It was found that aluminum alloy 2024 and 7075 grades would be corroded 0.039 and 0.061 mm each year. Although the Al7075 showed a higher strength, the corrosion rate was crucial which shortens the material lifespan.

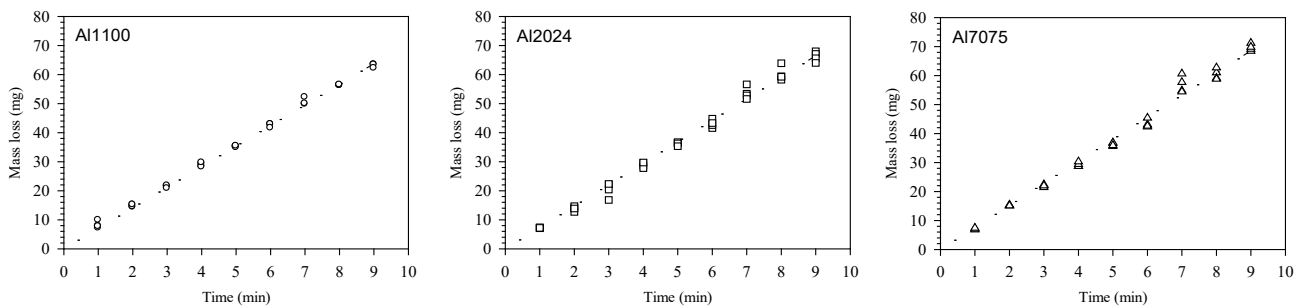


Figure 2. Mass loss of Al1100, Al2024, and Al7075 samples after electro-chemical etching at different etching time.

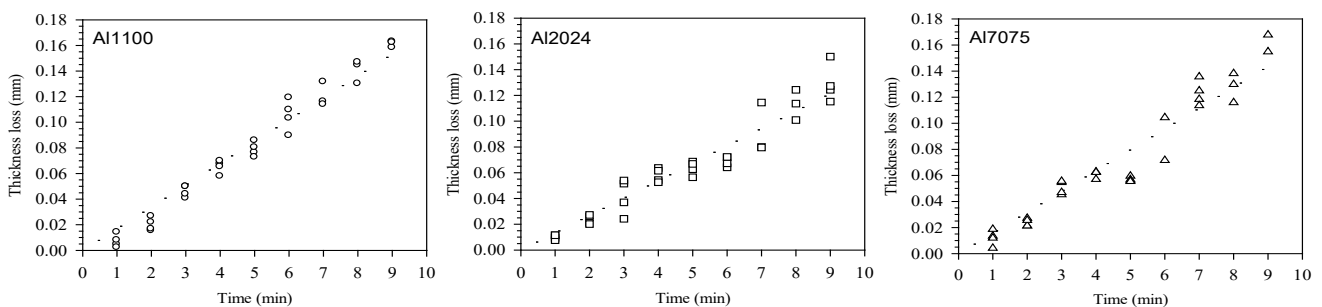
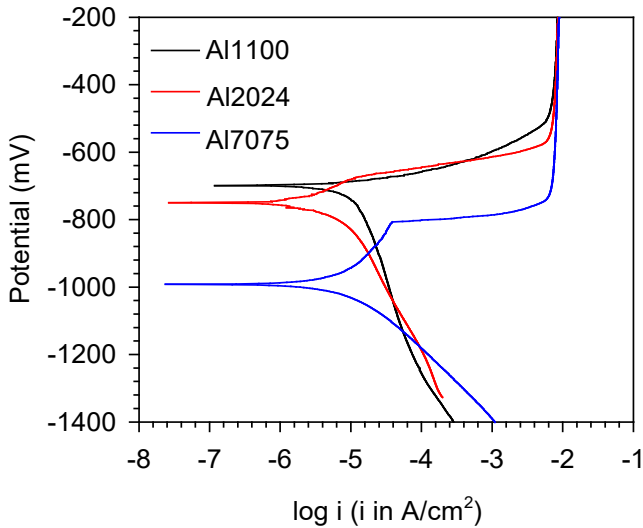


Figure 3. Thickness loss of Al1100, Al2024 and Al7075 samples after electrochemical etching at different etching times obtained from CMM measurement.

Table 1. Corrosion potential and corrosion rate of aluminum alloy 1100, 2024, and 7075 grade obtained from linear polarization curve.

Sample	Al1100	Al2024	Al7075
$E_{corr}$ (mV)	-741.1	-749.3	-990.5
$i_{corr}$ ( $\mu\text{A}\cdot\text{cm}^{-2}$ )	2.11	3.55	5.49
CR (mm/y)	0.023	0.039	0.061



**Figure 4.** Linear polarization curves of aluminum alloy 1100, 2024, and 7075 grade.

### 3.3 Eddy current testing results

The artificial corrosion damage was inspected using Mentor EM eddy current inspection device and reflection probe. For Al1100 materials, the first guess frequency was used as 1.811 kHz which was related to the first skin depth ( $\delta$ ) of material. The inspection results showed the 1.8 kHz frequency could detect all corrosion damage defects because the skin depth was set at 2 mm. which was thickness of material. This implies that the eddy current could penetrate to the other side of material but this frequency cannot estimate the depth of the thickness loss. However, to estimate the thickness loss, the frequency must be increased to shift the eddy current strength up to the surface [18].

Frequencies were guessed and shifted up until the peak amplitude of the result from each damage set is flat or indistinct from each other. Then, these frequencies were recorded and used for analysing the thickness loss estimation later. The thickness loss estimated frequencies for each set (1 min to 3 min, 4 min to 6 min, and 7 min to 9 min corrosion time) are 6.0, 6.4, and 6.8 kHz, respectively.

Figure 5 shows the results of all Al1100 specimen damages using time variation phase mode. This mode demonstrated the impedance change over inspection time. The peak amplitude showed the impedance change, the higher peak implies the deeper thickness loss due to corrosion.

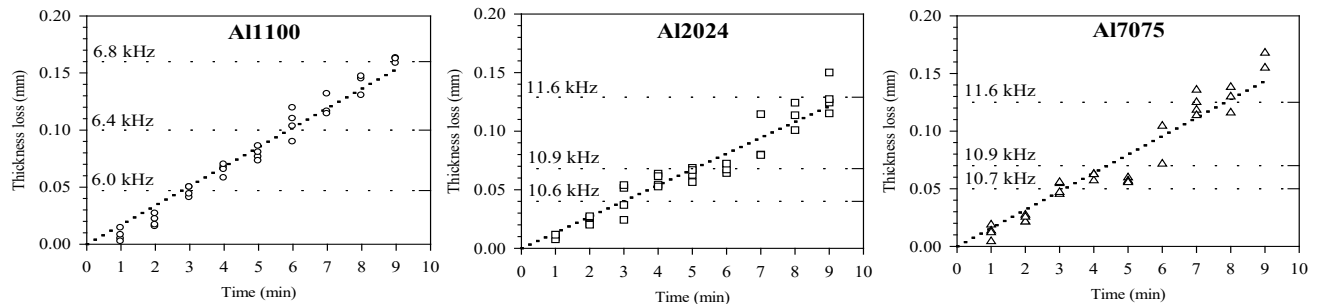


**Figure 5.** Corrosion damage thickness loss estimation and skin depth frequencies of materials Al1100, Al2024, and Al7075.

The results of Al2024 and Al7075 were also demonstrated in Figure 5. For Al2024 and Al7075, the material thickness frequencies were 3.3 kHz and 3.4 kHz. The conductivity of Al7075 was slightly lower than Al2024. The Al2024 has slightly lower frequencies than the Al7075. The frequencies for each plate of Al2024 were 10.6, 10.9, and 11.6 kHz, respectively. On the other hand, the Al7075 frequencies were 10.7, 10.9, and 11.6 kHz. All frequency results from thickness loss estimation were not related to the first skin depth ( $\delta$ ) but nearly the second skin depth ( $2\delta$ ) instead.

### 3.4 Thickness loss estimation of corrosion damage

The skin depth is depth from the surface that the eddy current strength has decayed to the strength value of  $1/e$  or around 37% signal penetration due to the Equation (3-5). Equation (5) is the solution of the differential Equation (3) which is derived from the Maxwell's Equation but considers only the conductor region  $z < 0$ . Eddy current density  $E(z)$  decays exponentially from maximum strength at the surface,  $E_x(0) = E_0$ . From the Equation (4), the skin depth is the inverse of the real part of the angular wave number  $k$  which is the distance determined by amount of wave, with the angular frequency  $\omega$ , packed in that region [18].

$$\left(\frac{d^2}{dz^2} - k^2\right) E_x(z) = 0, z < 0 \quad (3)$$

$$k = \sqrt{\frac{\omega\mu\sigma}{2}} (1+j) \quad (4)$$

$$E_x(z) = E_0 e^{(1+j)z/\delta}, \delta = \sqrt{\frac{2}{\omega\mu\sigma}} \quad (5)$$

From Equation (5), if the true depth ( $z$ ) is equal to  $\alpha\delta$  where the multiplier of the skin depth ( $\alpha$ ), such as  $\alpha=1$  for the first skin depth (37% signal penetration) and  $\alpha=2$  for the second skin depth (13% signal penetration). However, from calculation, the experimental results are related to non-integer multiplier of the skin depth. Actually, they are  $1.78\delta$  (16.9% signal penetration),  $1.75\delta$  (17.4% signal penetration) and  $1.74\delta$  (17.6% signal penetration) for Al 1100, Al2024 and Al7075 respectively. The signal penetration for each material is not equal according to Equation (2). It varies from the material conductivity, Al 1100 has highest conductivity followed by Al2024 and Al7075. The higher conductivity required lower signal penetration to estimate the thickness loss because the signal strength is higher.

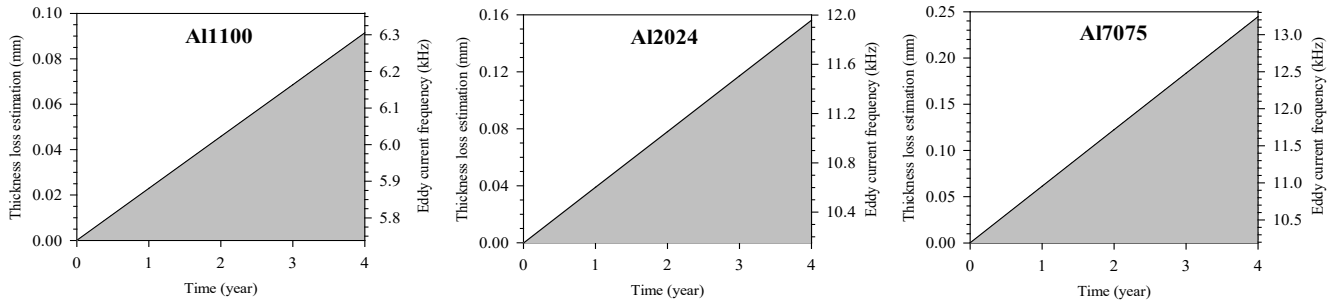


**Figure 6.** The material lifetime estimation from corrosion rate of materials Al1100, Al2024, and Al7075.

After the inspection process, the frequency results are calculated and analysed to estimate the corrosion damage thickness loss compare to the thickness loss measurement results from CMM. The results are also summarized in Figure 5. They show that when converting the frequency back to the thickness loss, all of the thickness loss estimations for every material are comparable to the measurement thickness loss. It can also imply that the thickness loss estimation has insignificantly error. These results can be concluded that the remaining thickness of sheet metal can be estimated by the skin depth even if the skin depth frequencies are varied with material conductivity

However, the skin depth still has to be guessed to match the real corrosion thickness loss but Equation (6) can aid the inspection. Equation (6) is the Equation (2) substituted by  $\delta = z / \alpha$  which can estimate true thick or thickness loss (material thickness minus  $z$ ). Equation (6) also explains the relation between eddy current probe frequency ( $f$ ) and true thickness loss. At the given set of material properties, the true thickness loss is proportional to the probe frequency. This probe frequency is represented by limited frequency criteria where the depth of the true thickness loss is shallow than that given probe frequency is undetectable but can still detect the deeper thickness loss. The inspector can choose these probe frequency criteria to identify the thickness loss. If the defect is undetectable at the given probe frequency, this implies that the corrosion has not occurred yet in that region or it is already corroded within the limit. However, this research also provides some suggestion that the corrosion rate from the potentiostat/galvanostat measurement could be used as the first estimation before affirm by the eddy current testing, which could reduce the inspection time.

$$f = \frac{1}{\pi \mu \sigma \left(\frac{z}{\alpha}\right)^2} \quad (6)$$

In Equation 7, the inspection interval or the material lifetime (MLT) can be determined by the thickness loss (TL) divided by corrosion rate (CR). Figure 6 is concluded the material lifetime (MLT) which is related to the thickness loss measurement in each corrosion damage and the suggested eddy current frequencies according to the thickness loss skin depth.

$$MLT = TL / CR \quad (7)$$

In industrial applications, the chart in Figure 7 can be used for by inspector to estimate the thickness loss and eddy current inspection frequency from corrosion rate line. At a given material lifetime, the chart shows the maximum eddy current frequency line for inspection.

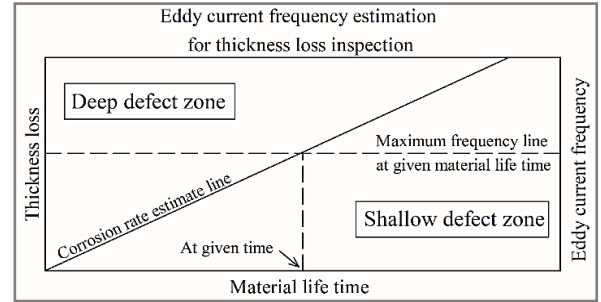


**Figure 7.** Eddy current frequency estimation for thickness loss inspection for industrial application.

If the defect is undetectable at this frequency, it implied that the defect is in the shallow defect zone, decreasing eddy current frequency is required to estimate the thickness loss. Contrastingly, if the defect is still detectable with higher frequency than this line, the defect is in the deep defect zone which implied that the thickness loss is higher than expected.

For inspection example, the inspector can determine the material life time using serial number traceability or maintenance schedule from the planning division. Then, the chart in Figure 6 can determine the thickness loss and the probe frequency criteria at the given material lifetime which can be used for the inspection process. From the inspection results, if the defect is undetectable, it implies that corrosion occurs within the limit which maintenance procedure does not require yet. But if the defect is detectable, it interprets that the corrosion is out of limit then the specimens have to be included under the maintenance process or rejected which also includes the thickness loss estimation information for maintenance method decision.

## 4. Conclusions

In this research, the artificial corrosion damage is created to estimate the thickness loss of materials Al1100, Al2024, and Al7075 using eddy current testing. The results are compared with the CMM measurement. They are shown that the corrosion thickness loss can be estimated using the eddy current skin depth frequencies. The guessing frequencies can be estimated using Equation (6) but the skin depth multiplier ( $\alpha$ ) can be determined by the experiment only with each material type. However, in the practical application, this research is suggested that the skin depth should be guessed from the corrosion rate thickness loss. Besides, the corrosion rate from the potentiostat-galvanostat measurement can also be estimated as the material lifetime for inspection interval.

## Credit author contribution statement

Seekharin Komonhirun: Conception and design of study, acquisition of data, analysis and interpretation of data, drafting the manuscript, revising the manuscript and approval of the manuscript to be published.

Sujittra Tangprakob: Contributed data and/or resources, analysis and interpretation of data, and approval of the manuscript to be published.

Sorawit Chanaphan: Contributed data and/or resources, analysis and interpretation of data, and approval of the manuscript to be published.

Awika Jaroensri: Contributed data and/or resources, analysis and interpretation of data, and approval of the manuscript to be published.

Thanasak Nilsonthi: Contributed data and/or resources and approval of the manuscript to be published.

Thammaporn Thublaor: Conception and design of study, acquisition of data, analysis and interpretation of data, drafting the manuscript, revising the manuscript and approval of the manuscript to be published.

## Acknowledgment

The authors sincerely thank the Department of Materials and Production Technology Engineering (MPTE), Dimensional Metrology and Calibration Center in Mechanical Engineering Technology Department, and Aircraft Maintenance Engineering Technology Workshop (ACET) in the Power Engineering Technology Department (PET) College of Industrial Technology (CIT) of the King Mongkut's University of Technology North Bangkok (KMUTNB) for facilities and instrumental supports. This research was funded by National Science, Research and Innovation Fund (NSRF) and King Mongkut's University of Technology North Bangkok (Contract no. KMUTNB-FF-65-09).

## Reference

- [1] J. R. Brence, and D.E. Brown, "Data mining corrosion from eddy current non-destructive tests," *Computer & Industrial Engineering*, vol. 43, pp. 821- 840, 2002.
- [2] J. Hernandez, Q. Fouliard, K. Vo, and S. Raghavan, "Detection of corrosion under insulation on aerospace structure via pulse eddy current thermography," *Aerospace Science and Technology*, vol. 121, p. 107317, 2022.
- [3] N. Yusa, and H. Hashizume, "Evaluation of stress corrosion cracking as a function of its resistance to eddy currents," *Nuclear Engineering and Design*, vol. 239, pp. 2713-2718, 2009.
- [4] N. Yusa, S. Perrin, and K. Miya, "Eddy current data for characterizing less volumetric stress corrosion cracking in nonmagnetic materials," *Materials letters*, vol. 61, pp. 827-829, 2007.
- [5] N. Yusa, L. Janousek, M. Rebican, Z. Chen, K. Miya, N. Dohi, N. Chiguasa, and Y. Matsumoto, "Caution when applying eddy current inversion to stress corrosion cracking," *Nuclear Engineering and Design*, vol. 236, pp. 211-221, 2006.
- [6] H. S. Shim, M. S. Choi, D. H. Lee, and D. H. Hur, "A prediction method for the general corrosion behavior of Alloy 690 steam generator tube using eddy current testing," *Nuclear Engineering and Design*, vol. 97, pp. 26-31, 2016.
- [7] K. Sodsai, M. Noipitak, V. Tangwarodomnukun, and C. Dumkum, "Probe designing for corrosion inspection under insulated surface by using eddy current method," *The Journal of Industrial Technology*, vol. 14, no. 2, N. pag. (in Thai), 2018.
- [8] H. Shaikh, N. Sivaibharasi, B. Sasi, T. Anita, R. Amirthalingam, B. P. C. Rao, T. Jayakumar, H. S. Khatak, and B. Raj, "Use of eddy current testing method in detection and evaluation of sensitization and intergranular corrosion in austenitic stainless steels," *Corrosion Science*, vol. 48, pp. 1462-1482, 2006.
- [9] Y. Li, B. Yan, D. Li, Y. Li, and D. Zhou, "Gradient-field pulsed eddy current probes for imaging of hidden corrosion in conductive structures," *Sensors and Actuators*, vol. 238, pp. 251-265, 2016.
- [10] N. Yusa, Z. Chen, K. Miya, T. Uchimoto, and T. Takagi, "Large-scale parallel computation for the reconstruction of natural stress corrosion cracks from eddy current testing signals," *NDT&E International*, vol. 36, pp. 449-459, 2003.
- [11] N. Yusa, and K. Miya, "Discussion on the equivalent conductivity and resistance of stress corrosion cracks in eddy current simulations," *NDT&E International*, vol. 42, pp. 9-15, 2009.
- [12] S. Hosseini, and A. A. Lakis, "Application of time-frequency analysis for automatic hidden corrosion detection in a multilayer aluminum structure using pulsed eddy current," *NDT&E International*, vol. 47, pp. 70-79, 2012.
- [13] Y. Li, B. Yan, D. Li, Y. Li, and Z. Chen, "Pulse-modulation eddy current inspection of subsurface corrosion in conductive structures," *NDT&E International*, vol. 79, pp. 142-149, 2016.
- [14] Y. He, G. Y. Tian, M. Pan, D. Chen, and H. Zhang, "An investigation into eddy current pulsed thermography for detection of corrosion blister," *Corrosion Science*, vol. 78, pp. 1-6, 2014.
- [15] H. M. G. Ramos, O. Postolache, F. C. Alegria, and A. L. Ribeiro, "Using the skin effect to estimate cracks depths in structures," *Instrumentation and Measurement Technology Conference*, N. pag, 2009.
- [16] ASTM Standard G102-89, "Standard practice for calculation of corrosion rates and related information from electrochemical measurements," *ASTM International*, West Conshohocken, PA, 2004.
- [17] ASTM Standard G1-03, "Standard Practice for Preparing, Cleaning, and Evaluating Corrosion Test Specimens," *ASTM International*, West Conshohocken, PA, 2004.
- [18] N. Bowler, *Eddy-current nondestructive evaluation*, 1<sup>st</sup> Ed., Springer Science + Business Media, NY, USA, 2019.
- [19] C. J. Hellier, *Handbook of nondestructive evaluation*, 1<sup>st</sup> Ed., The McGraw-Hill Companies, Inc., USA, 2003.
- [20] H. M. Obispo, L. E. Murr, R. M. Arrowood, and E. A. Trillo, "Copper deposition during the corrosion of aluminum alloy 2024 in sodium chloride solution," *Journal of Materials Science*, vol. 35, pp. 3479-3495, 2000.